Trajectory Tracking Control for Pneumatic Actuated Scan Stage with Time Delay Compensation

Wataru Ohnishi and Hiroshi Fujimoto
The University of Tokyo
5-1-5 Kashiwanoha, Kashiwa, Chiba, 277-8561 Japan
Phone: +81-4-7136-3873, +81-4-7136-4131
Email: ohnishi@hflab.k.u-tokyo.ac.jp, fujimoto@k.u-tokyo.ac.jp

Koichi Sakata, Atsushi Hara and Kazuaki Saiki
Nikon Corporation
471, Nagaodaityou, Sakae, Yokohama, 244-8533 Japan
Email: koichi.sakata@nikon.com
atsushi.hara@nikon.com
kazuaki.saiki@nikon.com

***Abstract*— A pneumatic actuator has several advantages such as low heat generation, high weight power ratio, and low cost. However, it has several disadvantages such as time delays and nonlinearities. Because pressure and position feedback bandwidths are limited by the time delay problem, it is difficult to implement a pneumatic actuator for a scan stage. Therefore, this paper proposes a modified Smith predictor for it and implements for an experimental scan stage. The effectiveness of the proposed control system is validated by frequency and time domain experiments.**

I. Introduction

High-precision stages are important machinery in the semiconductor and flat panel display manufacturing processes [1], [2]. To achieve the high integration and manufacturing cost reduction of electronic devices, faster and more precise positioning by larger stages are required. However, high speed positioning leads to increase in mass of the actuator. Therefore, this spurs on increase in the moving mass due to increase in the size of the stage. As a result, the heat generated by electromagnetic actuators is increased. Heat generation is a serious concern because it affects not only the proprieties of the mechanical system but also the proprieties of the actuation and measurement system [3], [4]. Another problem of increasing in the size and mass of the stage is a reduction in resonant frequency. Due to this problem, it is difficult to design a high bandwidth feedback controller. Hence, conventional scan stages face an inherent trade-offs between high throughput and high positioning accuracy [5].

To relax the trade-offs, a contactless dual stage structure which has a short stroke fine stage and a long stroke coarse stage is commonly used [6], [7]. This structure enables us to make a slightly lighter fine stage and reduce disturbance from the coarse stage. However, there is still limit to the reduction in the weight of the fine stage because the required maximum acceleration of the fine stage actuator is determined by the maximum acceleration of the setpoint trajectory. To deal with this problem, our group proposed the catapult stage [8], [9] which allows both contact and separation between the fine and coarse stages. The fine stage of the catapult stage is lighter and simpler compared to the conventional dual stage because the fine stage actuation is not necessary in the acceleration and deceleration region in the scanning motion.

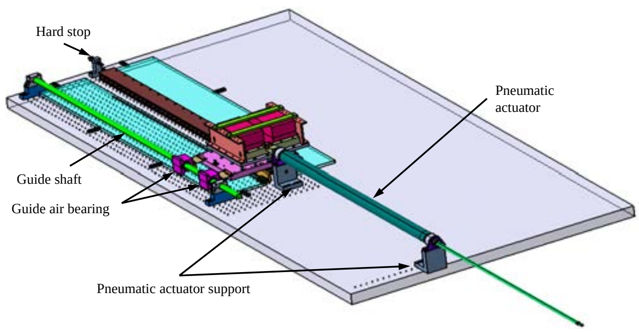

(a) Oblique view.

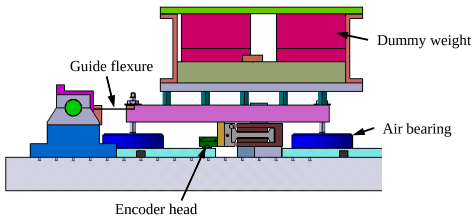

(b) Side view.

Fig. 1. Schematics of the pneumatic actuated scan stage.

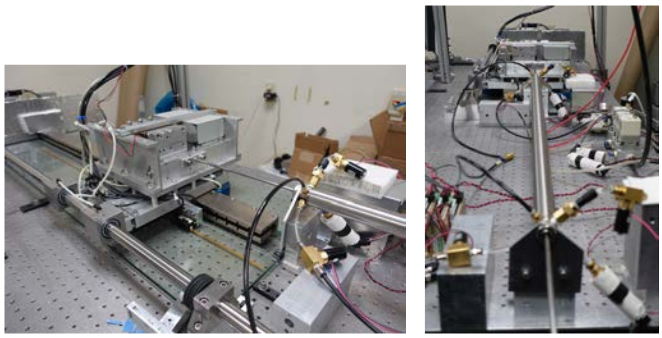

(a) Oblique view. (b) Side view.

Fig. 2. Photograph of the pneumatic actuated scan stage.

This paper considers a lightweight and simple structure for a coarse stage by replacing its linear motor to a pneumatic actuator. By combination of a catapult stage structure for fine stage and a pneumatic actuator for a coarse stage, a new generation dual stage with low heat generation, lightweight,

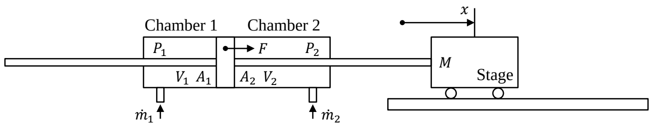

Fig. 3. Model of the pneumatic actuated scan stage.

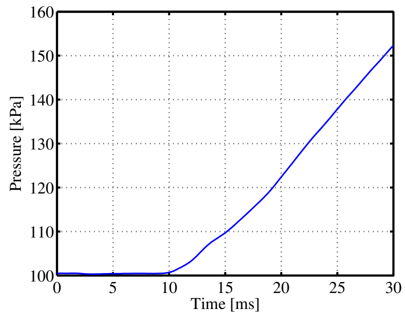

Fig. 4. Step response of the chamber 1. There is a delay from u_1^{ref} to P_{1m}.

and high positioning accuracy can be available. A pneumatic actuator has advantages compared to a linear motor: 1) low heat generation [4], 2) high weight power ratio [10], and 3) low cost [10]. Disadvantages are 1) the time delay [11] and 2) the nonlinearity dynamics [12], [13] due to air dynamics and servo valves. This paper focuses on the time delay problem which limits the feedback control bandwidth. Various methods have been studied for time delay problem: 1) Smith predictor [14] and its modifications [15], [16], 2) Internal Model Control (IMC) [17], and 3) communication disturbance observer [18]. This paper applies a modified Smith predictor to a trajectory tracking control problem.

Control methods for pneumatic actuators have been studied [19] including PID control [20], iterative leaning control [21], and sliding mode control [22]. Proposed control system of this paper has inner pressure feedback loops for each chamber with modified Smith predictors and an outer position feedback loop. The inner loops of this paper also have a pressure-derivative feedforward calculated by the jerk reference of the stage to improve the pressure tracking control performance.

II. Experimental Setup

Schematics and photographs of an experimental setup are shown in Fig. 1 and 2. This stage is designed as a miniaturized single axis (x) coarse stage actuated by a pneumatic cylinder. The coarse stage is supported by air pads to reduce friction. As illustrated in Fig. 3, the cylinder has two chambers. Each chamber has a pressure sensor, a high-pressure side poppet valve and an ambient side poppet valve. Supply air of the high-pressure side is 4×10^5 Pa. The position of the stage is measured by a linear encoder.

One of the problems of this pneumatic actuated stage is the time delay. Step response from the valve voltage reference in the chamber 1 to the measured pressure in the same chamber is shown in Fig. 4. There is a about 10 ms delay. This delay is not negligible to achieve high feedback bandwidths for the pressure and position feedback loops.

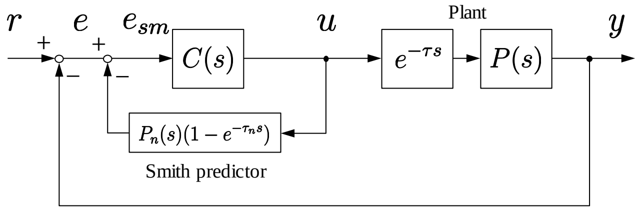

Fig. 5. Block diagram of the Smith predictor.

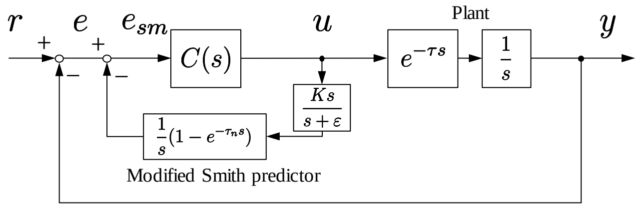

Fig. 6. Block diagram of the modified Smith predictor.

III. Time Delay Compensation by Modified Smith Predictor

A. Smith predictor

This subsection introduces the Smith predictor [14]. This section assumes a plant with input delay $P(s)e^{-\tau s}$. Without Smith predictor, the tracking control performance is

$$\frac{y(s)}{r(s)} = \frac{C(s)P(s)e^{-\tau s}}{1 + C(s)P(s)e^{-\tau s}}. \tag{1}$$

The denominator of (1) has a delay element which deteriorates a feedback stability. With the Smith predictor shown in Fig. 5, the tracking control performance becomes

$$\frac{y(s)}{r(s)} = \frac{C(s)P(s)e^{-\tau s}}{1 + C(s)P(s)} \tag{2}$$

when $P_n(s) = P(s)$ and $\tau_n = \tau$. Because the denominator of (2) does not have a delay element, the feedback controller $C(s)$ can be designed as a system without delay.

B. Modified Smith predictor and its analysis

However, the Smith predictor cannot be used for an unstable system or an integrating system with a constant disturbance [16]. To deal with this problem, this paper proposes a modified Smith predictor with a high pass filter (HPF) illustrated in Fig. 6 for the integrating system. Fig. 6 has two tuning parameters: a cut off frequency of the HPF ε and a gain K.

Step responses and frequency characteristics are analyzed. Conditions of this analysis for the modified Smith predictor are as follows. Plant is defied as $P(s) = \frac{1}{s}e^{-\tau s}$ which has an input delay $\tau = 10$ ms. A feedback controller $C(s)$ is designed as PI controller. Gain is set to locate the closed loop poles at -20Hz without considering the delay. In this case, the feedback loop is unstable without the Smith or modified Smith predictor.

In Fig. 7–9, ‘Smith’ denotes the standard Smith predictor case shown in Fig. 5. The others denote methods with the modified Smith predictor.

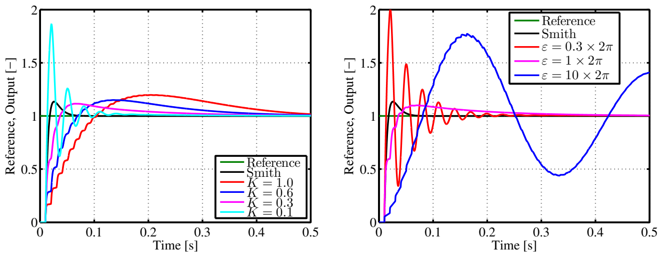

(a) Change K. ($\varepsilon = 1{\times}2\pi$, fixed) (b) Change ε. ($K = 0.3$, fixed)

Fig. 7. Step reference responses of the modified Smith predictor

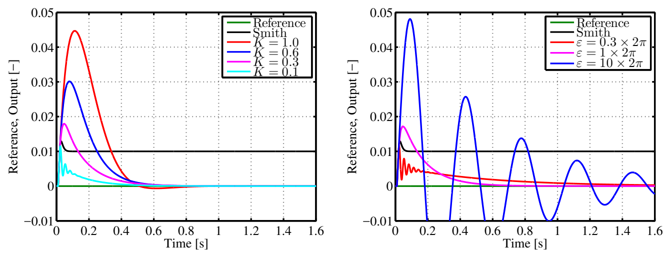

(a) Change K. ($\varepsilon = 1{\times}2\pi$, fixed) (b) Change ε. ($K = 0.3$, fixed)

Fig. 8. Disturbance step reference responses of the modified Smith predictor

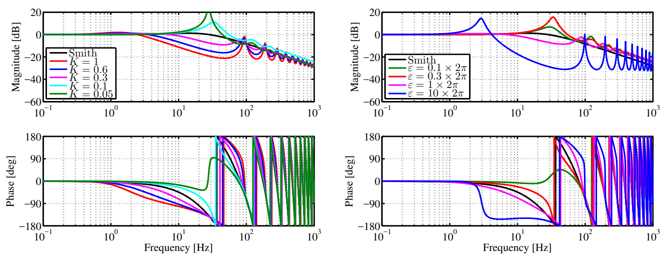

(a) Change K. ($\varepsilon = 1{\times}2\pi$, fixed) (b) Change ε. ($K = 0.3$, fixed)

Fig. 9. Frequency analysis $\frac{y(s)}{r(s)}$ of the modified Smith predictor

1) Step responses: The unit step responses for r is shown Fig. 7. Fig. 7(a) shows the less K is, the faster the response is. Fig. 7(a) depicts that smaller ε contributes higher response speed. However, too small K and ε case shows a big overshoot.

2) Disturbance responses: The unit input disturbance responses are shown in Fig. 8. The standard Smith predictor case, the steady state error is inevitable because the plant and the Smith predictor have an integrator. Fig. 8(a) shows the less K is, the faster response is. Fig. 8(b) depicts that smaller ε contributes higher response speed. However, too small ε case requires longer convergence time.

C. Frequency analysis

The bode diagrams of closed loop are shown in Fig. 9. Fig. 9(a) shows that small K improves the closed loop performance. In too small K case ($K = 0.05$), the closed loop becomes unstable. Fig. 9(b) depicts that small ε helps improvement of the closed loop performance.

IV. Modeling

The model of the pneumatic actuated stage is illustrated in Fig. 3. Block diagram of overall control system is shown in Fig. 10. Gas equation is expressed as

$$P_i(t)V_i(t) = m_i(t)RT_i, \tag{3}$$

where P_i, V_i, m_i, R, T_i denotes chamber pressure, chamber volume, mass of the gas, ideal gas constant, temperature for each chambers, respectively. Chamber temperature T_i is assumed as a constant. The subscript i represents the chamber number. By time differentiation of (3),

$$\dot{P}_i(t)V_i(t) + P_i(t)\dot{V}_i(t) = \dot{m}_i(t)RT_i \tag{4}$$

is obtained. From (4), $\dot{P}_i$ is modeled as

$$\dot{P}_i(t) = \frac{-P_i(t)\dot{V}_i(t) + \dot{m}_i(t)RT_i}{V_i(t)}. \tag{5}$$

A nonlinear model NL from valve commands $u_{i,in}, u_{i,out}$ to $\dot{m}_i$ shown in Fig. 10 is obtained by polynomial fitting of experimental data [12].

Equation of motion of the stage is

$$\begin{aligned} f(t) &= P_1(t)A - P_2(t)A \\ &= M\ddot{x}(t), \end{aligned} \tag{6}$$

where f, A, M, x denotes the force from the pneumatic cylinder, the size of the pressurized area, the mass, and the position of the stage, respectively.

V. Basic Control System

Basic control system of the pneumatic actuation stage is shown in Fig. 10. As an inner loop, a pressure feedback is implemented for each chamber. As an outer loop, a position feedback is implemented for stage position by using a linear encoder.

A. Position control

$C^x_{fb}(s)$ is implemented as an outer loop position feedback controller. The relationship between the output of position feedback f^{ref} and the pressure commands P_1^{ref}, P_2^{ref} is

$$P_1^{ref}(t) = P^{set} + \frac{f^{ref}(t)}{2A}, \quad P_2^{ref}(t) = P^{set} - \frac{f^{ref}(t)}{2A}, \tag{7}$$

where P^{set} denotes the set pressure for each chamber. In this case, P^{set} is set as 2.0×10^5 Pa. $C^x_{fb}(s)$ is designed by a series connection of a PI controller, a phase lead filter, and notch filters.

B. Pressure control

Pressure feedback controllers C^{P1}_{fb}, C^{P2}_{fb} are designed as a series connection of a PI controller, a phase lead filter, and notch filters.

The reference of the derivative of the gass mass is obtained as follows:

$$\dot{m}_i^{ref}(t) = \frac{\dot{P}_i^{ref}(t)V_i(t) + P_i(t)\dot{V}_i(t)}{RT_i}. \tag{8}$$

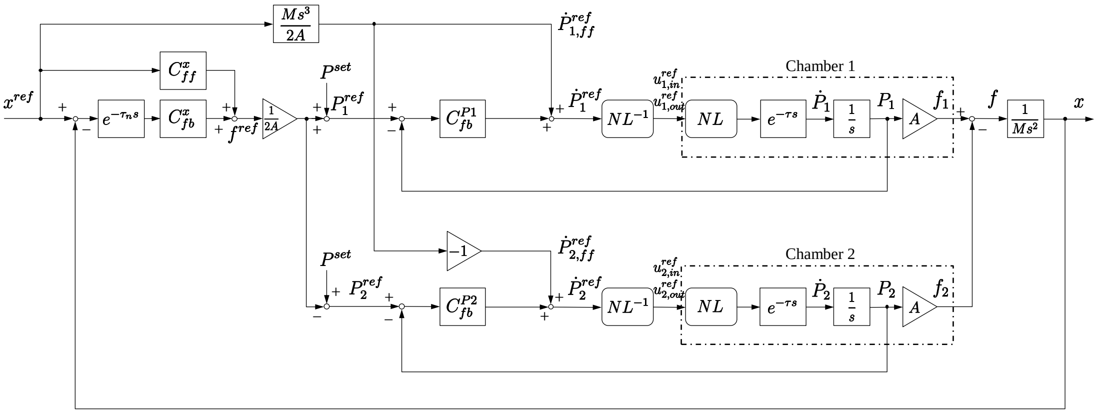

Fig. 10. Block diagram of the conventional control system.

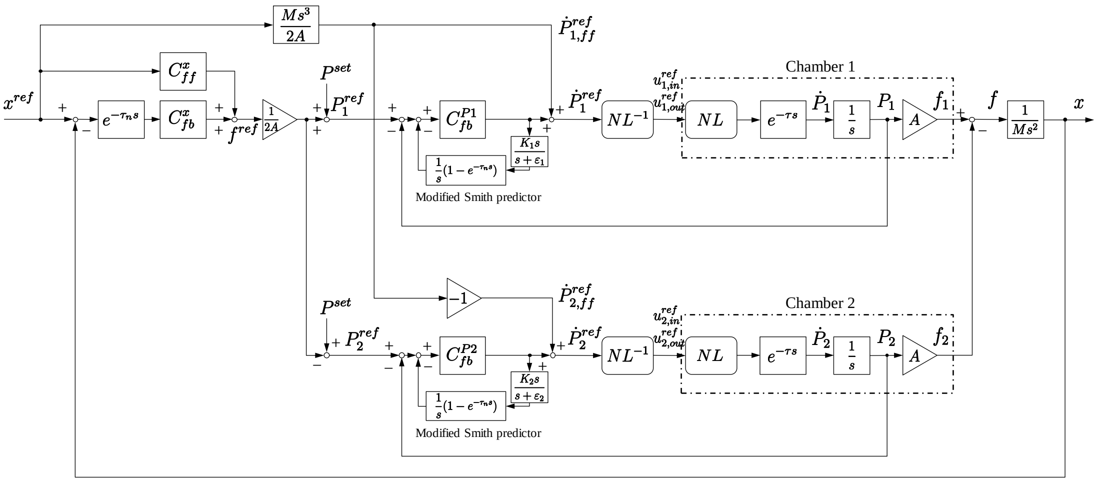

Fig. 11. Block diagram of the proposed control system.

An inverse model NL^{-1} from $\dot{m}_i^{ref}$ to $u_{i,in}^{ref}, u_{i,out}^{ref}$ is calculated by inverse of the polynomial obtained in subcsection IV.

Feedforward commands $\dot{P}_{1,ff}^{ref}, \dot{P}_{2,ff}^{ref}$ are obtained by deferential of (6) and (7):

$$\dot{P}_{1,ff}^{ref}(t) = \frac{M\dddot{x}^{ref}(t)}{2A}, \quad \dot{P}_{2,ff}^{ref}(t) = -\frac{M\dddot{x}^{ref}(t)}{2A}. \tag{9}$$

VI. Experimental Results

A. Pressure feedback

The case 1 and case 2 are performed by the block diagrams shown in Fig. 10 and Fig. 11, respectively. Pressure feedback control performance is shown in Fig. 12 and Tab. I. In case 1, C_{fb}^{P1}, C_{fb}^{P2} are designed to have about 35 degree phase margin without the modified Smith predictor. In case 2, C_{fb}^{P1}, C_{fb}^{P2} are redesigned to have about 35 degree phase margin with the modified Smith predictor. The parameters of the Modified Smith predictor are set as $\tau_n = 10\,\mathrm{ms}$, $K_1 = 0.3$, $K_2 = 0.4$, and $\varepsilon = 1 \times 2\pi\,\mathrm{rad/s}$.

Fig. 12 shows a frequency response from the force command for the pneumatic cylinder f^{ref} to estimated force generated by the pneumatic cylinder $\hat{f}$. $\frac{\hat{f}(j\omega)}{f^{ref}(j\omega)}$ is calculated by

$$\frac{\hat{f}(j\omega)}{f^{ref}(j\omega)} = \frac{P_1(j\omega)A - P_2(j\omega)A}{f^{ref}(j\omega)}. \tag{10}$$

In Tab. I, the bandwidth is defined as -90 degree crossover of $\frac{\hat{f}(j\omega)}{f^{ref}(j\omega)}$. From Fig. 12 and Tab. I, the pressure feedback bandwidth is improved from 9.4 Hz to 31 Hz regardless of similar phase margin.

B. Position feedback

Frequency response of the position feedback is shown in Fig. 13 and Tab. II. In the case 1, the phase margin of position feedback is 22 degree. In the case 2, the phase margin of position feedback is 53 degree because the inner loop pressure feedback is improved. In the case 3, the outer loop position feedback controller C_{fb}^{x} is redesigned. The position feedback bandwidth is improved from 5.3 Hz to 11 Hz although the gain and phase margins increase.

Time responses are shown in Fig. 14. In this experiment, a scan trajectory is given as a reference shown in Fig. 14(a). Tracking performances are depicted in Fig. 14(b), (c). In the case 3, the maximum tracking error is improved from 507.7

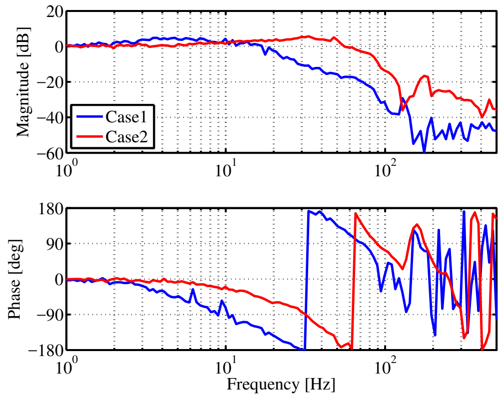

Fig. 12. Pressure feedback control performance $\frac{\hat{f}(j\omega)}{f^{ref}(j\omega)}$ calculated by (10).

TABLE I
PRESSURE FEEDBACK CONTROL PERFORMANCE BY FIG. 12.

	Case1	Case2
Pressure FB	low gain	high gain + MSP*
Gain margin	13dB (32Hz)	6.4dB (62Hz)
Phase margin	35deg (6.9Hz)	35deg (27Hz)
Bandwidth	9.4Hz	31Hz

*Modified Smith predictor

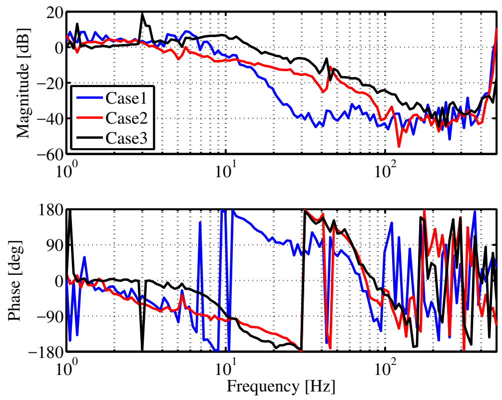

Fig. 13. Position control performance $\frac{x(j\omega)}{x^{ref}(j\omega)}$.

TABLE II
POSITION FEEDBACK CONTROL PERFORMANCE BY FIG. 13.

	Case 1	Case 2	Case 3
Pressure FB	low gain	high gain + MSP*	same as case 2
Position FB	low gain	same as case 1	high gain
Gain margin (Position FB)	7.0dB (9Hz)	17dB (30Hz)	9.6dB (30Hz)
Phase margin (Position FB)	22deg (5.9Hz)	53deg (3.2Hz)	26deg (10Hz)
Bandwidth (Position FB)	5.3Hz	7.7Hz	11Hz

*Modified Smith predictor

μm to 135.3 μm because the case 3 has a high bandwidth feedback controller.

VII. CONCLUSION

This paper investigate a pneumatic actuator for a scan stage to replace a linear motor. A pneumatic actuator has advantages such as low heat generation, high weight power ratio, and low cost. On the other hand, it has disadvantages such as a time delay and a nonlinearity. Due to the time delay problem, it is difficult to implement the high bandwidth feedback controller.

The proposed control system has pressure feedback inner loops for each chamber and a position feedback outer loop. The nominal plant of the inner loop is an integrator. The standard Smith predictor can not be used in a system with an integrator. Therefore, this paper proposes a modified Smith predictor and implements to an experimental scan stage.

The proposed control system with the modified Smith predictor in the inner loops can achieve high bandwidths for inner loops and outer loop. Time response data indicate high position tracking performance.

ACKNOWLEDGMENT

The contributions of Nikon Research Corporation of America are gratefully acknowledged. This work is supported by JSPS KAKENHI Grant Number 15J08488.

REFERENCES

[1] H. Butler, "Position Control in Lithographic Equipment," *IEEE Control Systems Magazine*, vol. 31, no. 5, pp. 28–47, 2011.

[2] K. Saiki, A. Hara, K. Sakata, and H. Fujimoto, "A Study on High-Speed and High-Precision Tracking Control of Large-Scale Stage Using Perfect Tracking Control Method Based on Multirate Feedforward Control," *IEEE Transactions on Industrial Electronics*, vol. 57, no. 4, pp. 1393–1400, 2010.

[3] Y. Choi and D. Gweon, "A high-precision dual-servo stage using halbach linear active magnetic bearings," *IEEE/ASME Transactions on Mechatronics*, vol. 16, no. 5, pp. 925–931, 2011.

[4] T. Kagawa, K. Sakaki, L. R. Tokashiki, and T. Fujita, "Accurate Positioning of a Pneumatic Servo System With Air Bearings," in *Proceedings of the JFPS International Symposium on Fluid Power*, pp. 693–698, 2002.

[5] K. Sakata, H. Asaumi, K. Hirachi, K. Saiki, and H. Fujimoto, "Self Resonance Cancellation Techniques for a Two-Mass System and Its Application to a Large-Scale Stage," *IEEJ Journal of Industry Applications*, vol. 3, no. 6, pp. 455–462, 2014.

[6] M. F. Heertjes, "Variable Gains in Motion Control of Wafer Scanners," *IEEJ Journal of Industry Applications*, vol. 5, no. 2, pp. 90–100, 2015.

[7] W. Ohnishi, H. Fujimoto, K. Sakata, K. Suzuki, and K. Saiki, "Decoupling Control Method for High-Precision Stages using Multiple Actuators considering the Misalignment among the Actuation Point, Center of Gravity, and Center of Rotation," *IEEJ Journal of Industry Applications*, vol. 5, no. 2, pp. 141–147, 2016.

[8] Y. Yazaki, H. Fujimoto, K. Sakata, A. Hara, and K. Saiki, "Settling time shortening method using final state control for high-precision stage with decouplable structure of fine and coarse parts," in *40th Annual Conference of the IEEE Industrial Electronics Society*, pp. 2859–2865, 2014.

[9] Y. Yazaki, H. Fujimoto, K. Sakata, A. Hara, and K. Saiki, "Application of Mode Switching Control Using Initial State Variables in Constraint Final-State Control to High-Precision Dual Stage," in *American Control Conference*, pp. 4155–4161, 2015.

[10] I. Ramírez, "Modeling and tracking control of a pneumatic servo positioning system," in *2013 2nd International Congress of Engineering Mechatronics and Automation*, pp. 1–6, 2013.

[11] Y. Nakamura, H. Kawakami, and S. Wakui, "Suppression of Anti-Resonance and Resonance in Pneumatic System of Vibration Isolator Considering Time Delay," in *41st Annual Conference of the IEEE Industrial Electronics Society*, pp. 2509–2514, 2015.

[12] Z. Rao and G. M. Bone, "Nonlinear modeling and control of servo pneumatic actuators," *IEEE Transactions on Control Systems Technology*, vol. 16, no. 3, pp. 562–569, 2008.

[13] A. C. Valdiero, C. S. Ritter, C. F. Rios, and M. Rafikov, "Nonlinear mathematical modeling in pneumatic servo position applications," *Mathematical Problems in Engineering*, vol. 2011, 2011.

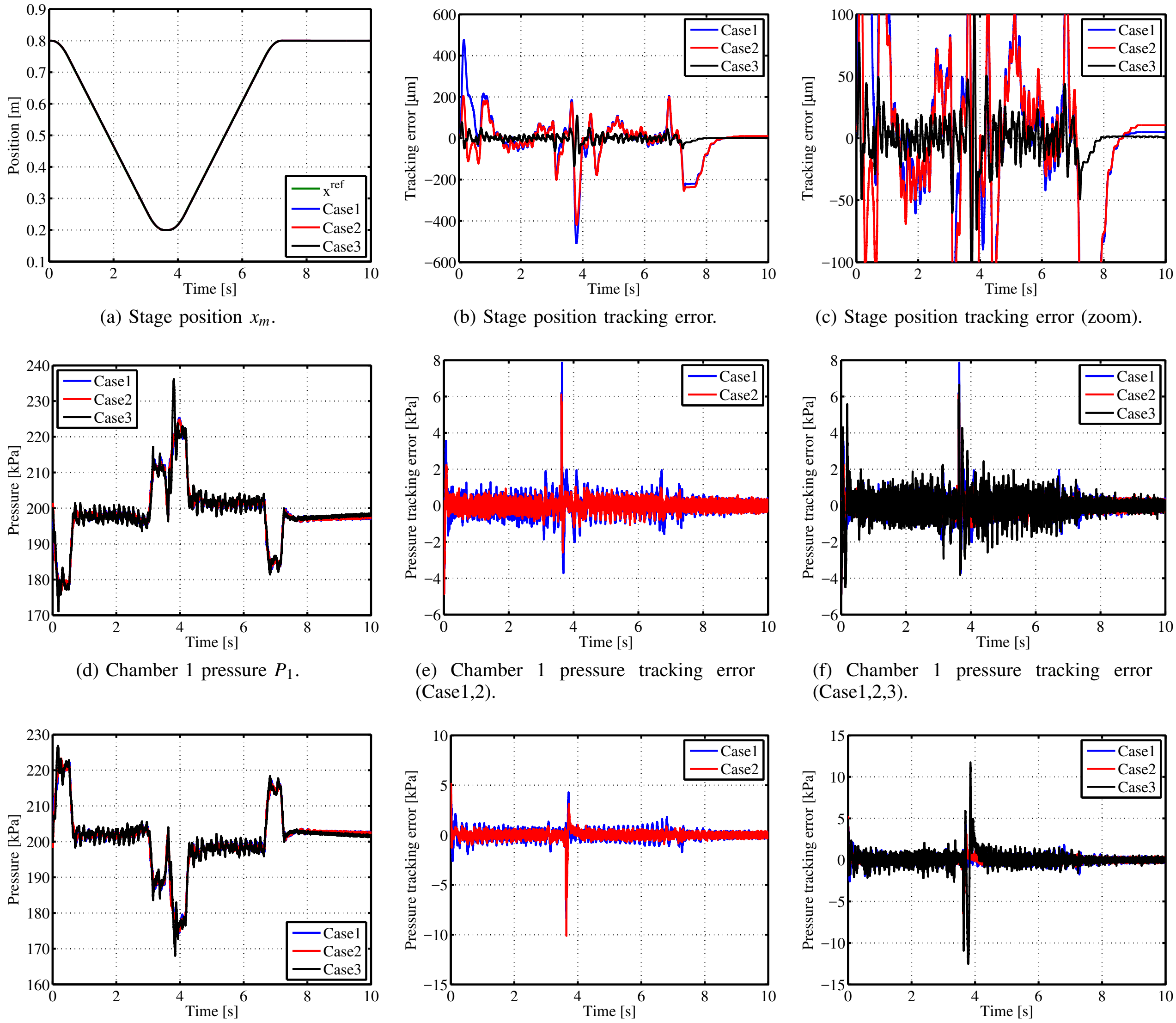

(a) Stage position x_m.

(b) Stage position tracking error.

(c) Stage position tracking error (zoom).

(d) Chamber 1 pressure P_1.

(e) Chamber 1 pressure tracking error (Case1,2).

(f) Chamber 1 pressure tracking error (Case1,2,3).

(g) Chamber 2 pressure P_2.

(h) Chamber 2 pressure tracking error (Case1,2).

(i) Chamber 2 pressure tracking error (Case1,2,3).

Fig. 14. Scan motion experimental results.

TABLE III

SCAN MOTION EXPERIMENTAL RESULTS BY FIG. 14.

	Case1	Case2	Case3
Max error (Ch1, Pressure)	7.9 [kPa]	6.1 [kPa]	6.6 [kPa]
Max error (Ch2, Pressure)	8.4 [kPa]	10.1 [kPa]	12.5 [kPa]
Max error (Position)	507.7 [um]	417.8 [um]	135.3[um]

[14] O. J. M. Smith, “A Controller to Overcome Dead Time,” *Indian Scientist Association in Japan*, vol. 6, no. 2, pp. 28–33, 1959.

[15] K. Watanabe and M. Ito, “A process-model control for linear systems with delay,” *IEEE Transactions on Automatic Control*, vol. 26, no. 6, pp. 1261–1269, 1981.

[16] K. Åström, C. Hang, and B. Lim, “A new Smith predictor for controlling a process with an integrator and long dead-time,” *IEEE Transactions on Automatic Control*, vol. 39, no. 2, pp. 343–345, 1994.

[17] M. Morari and E. Zafiriou, *Robust Process Control*. Prentice Hall, 1989.

[18] K. Natori and K. Ohnishi, “A design method of communication disturbance observer for time-delay compensation, taking the dynamic property of network disturbance into account,” *IEEE Transactions on Industrial Electronics*, vol. 55, no. 5, pp. 2152–2168, 2008.

[19] M. Rahmat, N. H. Sunar, S. N. S. Salim, M. S. Z. Abidin, a. a. M. Fauzi, and Z. H. Ismail, “Review on Modeling and Controller Design,” *International Journal on Smart Sensing and Intelligent Systems*, vol. 4, no. 4, pp. 630–661, 2011.

[20] R. B. Van Varseveld and G. M. Bone, “Accurate position control of a pneumatic actuator using on/off solenoid valves,” *IEEE/ASME Transactions on Mechatronics*, vol. 2, no. 3, pp. 195–204, 1997.

[21] C. K. Chen and J. Hwang, “Iterative learning control for position tracking of a pneumatic actuated X-Y table,” *Control Engineering Practice*, vol. 13, no. 12 SPEC. ISS., pp. 1455–1461, 2005.

[22] Y. C. Tsai and A. C. Huang, “Multiple-surface sliding controller design for pneumatic servo systems,” *Mechatronics*, vol. 18, no. 9, pp. 506–512, 2008.